Surface-enhanced Raman scattering properties of highly ordered self-assemblies of gold nanorods with different aspect ratios*

Shi Xue-Zhao(时雪钊)[a)b)], Shen Cheng-Min(申承民)[b)], Wang Deng-Ke(王登科)[b)c)], Li Chen(李 晨)[b)], Tian Yuan(田 园)[b)], Xu Zhi-Chuan(徐桎川)[b)], Wang Chun-Ming(王春明)[a)†], and Gao Hong-Jun(高鸿钧)[b)‡]

[a)] *College of Chemistry and Engineering, Lanzhou University, Lanzhou* 730000, *China*
[b)] *Institute of Physics, Chinese Academy of Sciences, Beijing* 100190, *China*
[c)] *School of Physical Science and Technology, Yunnan University, Kunming* 650091, *China*

(Received 1 March 2011; revised manuscript received 13 April 2011)

Gold nanorods with aspect ratios of from 1 (particles) to 31.6 were synthesized by the seed-mediated method and packed in a highly ordered structure on a large scale on silicon substrates through capillary force induced self-assembly behaviour during solvent evaporation. The gold nanorod surface exhibits a strong enhancing effect on Raman scattering spectroscopy. The enhancement of Raman scattering for two model molecules (2-naphthalenethiol and rhodamine 6G) is about 5–6 orders of magnitude. By changing the aspect ratio of the Au nanorods, we found that the enhancement factors decreased with the increase of aspect ratios. The observed Raman scattering enhancement is strong and should be ascribed to the surface plasmon coupling between closely packed nanorods, which may result in huge local electromagnetic field enhancements in those confined junctions.

Keywords: gold nanorods, surface plasmon resonance, self assemble, surface enhanced Raman scattering

PACS: 61.46.Km, 74.25.nd, 78.67.Qa, 87.64.kp **DOI:** 10.1088/1674-1056/20/7/076103

1. Introduction

Gold and silver nanostructures show excellent surface plasmon resonance (SPR) properties, which make them very promising for optical biosensors,[1−3] surface-enhanced Raman scattering (SERS)[4−6] and photothermal therapy.[7,8] Among these, SERS, using Au or Ag nanostructures as substrates, is a powerful analytical tool for collecting the molecular chemical information.[9] Many studies have revealed that SERS can be observed for molecules adsorbed on the surface of isolated metal nanostructures.[10−15] However, strong SERS behaviour occurs only when the metal nanostructure is packed closely. An enhanced electric field occurs at the gap between closely packed nanostructures when the nanostructures are illuminated with light at their SPR wavelength, and those gaps where nanostructures contact are more effective locations for SERS.[16] Therefore, the packing of nanostructures plays a crucial role for strong SERS signals and much effort has been made to build highly ordered Au or Ag packing nanostructures in order to increase SERS sensitivity.[17−22]

Recently, one-dimensional nanostructures, such as gold nanorods and nanowires, have attracted great attention due to their tunable longitudinal plasmon absorption and scattering properties.[23−28] Some studies have demonstrated that one-dimensional Au and Ag nanostructures can be used as substrates in order to improve SERS sensitivity.[29,30] They were also used to enhance the SERS in an aqueous solution via the overlap of longitudinal plasmon resonance with the excitation source.[31] A sandwich architecture structure with molecules immobilized between the plane substrate and the Au nanostructures shows high enhancement effect.[32] Compared with those

*Project supported by the National Natural Science Foundation of China (Grant No. 50872147), the National High Technology Research and Development Program of China (Grant No. 2007AA03Z305), and the Special Doctoral Foundation of the Ministry of Education of China (Grant No. 20775030).

†Corresponding author. E-mail: cmwang@lzu.edu.cn
‡Corresponding author. E-mail: hjgao@aphy.iphy.ac.cn

works, there are few reports on the SERS behaviours of highly ordered closely packed Au nanorods. In this paper, we study the dependence of the SERS effect on the aspect ratios of highly ordered Au nanorod assemblies, which were synthesized and packed on silicon substrate. The SERS-enhancing properties of these nanorod assemblies were investigated using 2-naphthalenethiol (2-NAT) and Rhodamine 6G (R6G) as model molecules. We found that the assembly of Au nanorods with the aspect ratio of 7.8 is most effective for SERS-enhancement, even at low concentrations of model molecules.

2. Experiment

2.1. Materials

Silver nitrate, cetyltrimethylammonium bromide (CTAB), ascorbic acid, sodium borohydride and 2-naphthalenethiol (2-NAT) were purchased from Aldrich. Chloroauric acid, Rhodamine 6G (R6G) and tri-sodium citrate dihydrate were purchased from the Beijing Chemical Reagent Company. All chemicals were used without further purification.

2.2. Synthesis of different aspect ratio Au nanorods

Gold nanorods were synthesized by the seed mediated method developed by Jana's group.[33,34] For seed preparation, a 20-mL aqueous solution containing 2.5×10^{-4} M $AgNO_3$ and 2.5×10^{-4} M tri-sodium citrate was prepared. Then 0.50 mL of ice cold 0.10 M $NaBH_4$ solution was added with stirring. The solution colour turned to orange immediately and stirring was continued for 20 s after adding $NaBH_4$, and the seed solution should be used within 2–8 h after preparation. For the nanorod growth, a one-step procedure is employed here. Four conical flasks, each containing 10 mL growth solution consisting of 2.5×10^{-4} M $HAuCl_4$ and 0.10 M CTAB, were mixed with 100 μL 0.05 M of freshly prepared ascorbic acid aqueous solution. Ascorbic acid as a mild reducing agent changing the growth solution colour from brown-yellow to colorless signifies that gold has been reduced from Au (III) to Au (I)-CTAB complex. Next, a series of seed solutions in different volumes, 1.0, 2.5, 5.0 and 20.0 μL, were added into the four conical flasks, respectively. While for the fourth conical flask, stirring was continued until the reaction was stopped by removing the growth solution through centrifugation. After half an hour, all the solutions were dark wine red in color. For the rod sample, the resulting supernatant was carefully removed and the film on the bottom was carefully rinsed with a small portion of double distilled water to remove the residual amount of the supernatant. While, for the particles, centrifugation at 6000 rpm for 10 min was needed to remove excess surfactant. The as-prepared sample was washed three times using double distilled water and redispersed into 1 mL water.

2.3. Fabrication of nanorod assemblies and preparation of SERS samples

The highly ordered Au nanorod assemblies were fabricated as in our previous work.[35] A 10-μL aqueous dispersion of Au nanorods was dropped onto cleaned 0.50 cm×0.50 cm silicon wafers, which were already positioned in a closed vessel. A small flask with water was placed in the same vessel to slow down the solvent's evaporation. The dried samples were investigated by a field emission scanning electron microscope and were used as SERS substrates. Then 20 μL of model-molecule ethanol solutions were dropped onto the assembled nanorod substrates for SERS measurement after the solvent had evaporated. All the samples were rinsed three times with absolute alcohol to wash away the remnant molecules.

2.4. Characterizations of Au nanorods

A field emission scanning electron microscope (FE-SEM, XL30 S-FEG, FEI Corp. at 10 kV) was used to observe the morphology of the samples. Transmission electron microcopy (TEM) images were acquired with a Tecnai-20 (PHILIPS Cop) at 200 kV. The UV-Vis absorption spectra of the samples were recorded by a Cary IE UV-Vis spectrometer. X-ray diffraction patterns were collected on a Rigaku D/MAX 2400 X-ray diffractometer with CuKα1 radiation (λ = 1.5406 Å). The surface-enhanced Raman spectra and Raman mapping were recorded on a Raman system YJ-HR800 with confocal microscopy. A solid-state diode laser (785 nm) was used as the excitation source and the laser power on the samples was kept at 0.7 mW.

3. Results and discussion

3.1. Synthesis of gold nanorods and their assemblies

Figure 1 shows typical SEM images of gold nanorod assemblies with different aspect ratios. The

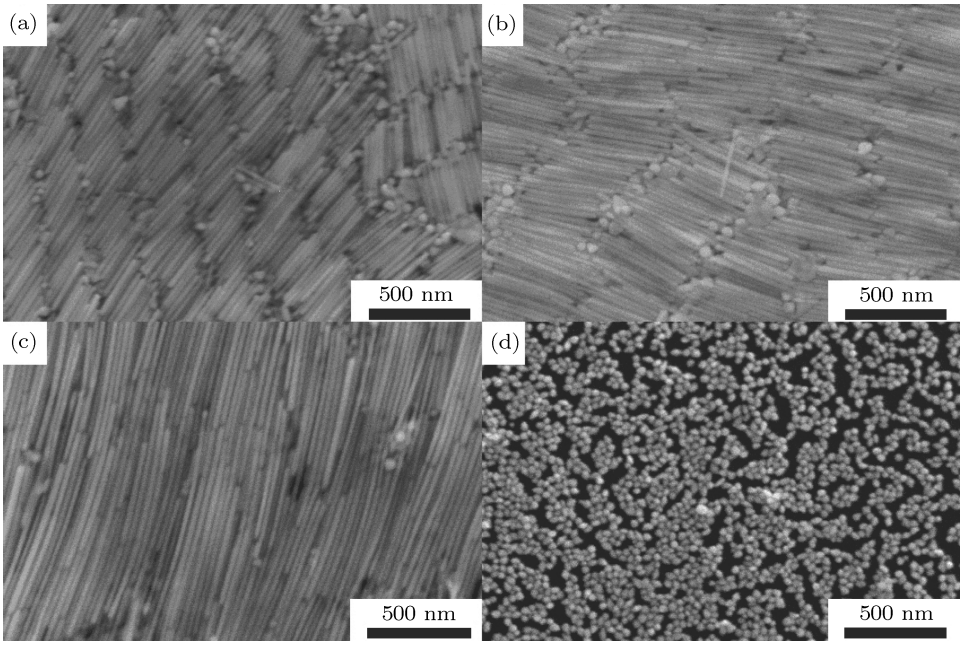

Fig. 1. SEM images of gold nanorod self-assemblies with different aspect ratios: (a) about 29 nm in diameter and about 227 nm in length, (b) about 27 nm in diameter and about 400 nm in length, (c) about 27 nm in diameter and about 850 nm in length. (d) Gold nanoparticles with a diameter of about 30 nm. The SEM images show that the Au nanorod sample forms highly ordered self-assemblies on a large scale through capillary force.

diameter of the obtained nanorods was between 27 nm and 30 nm, and the length ranged from 850 nm to 227 nm. By providing a humid environment, the evaporation rate of the Au nanorod solutions was slowed effectively in order to allow the formation of ordered packing structures of Au nanorods. These Au nanorods aligned side by side in a highly ordered ribbon structure and the ribbon structures were packed closely with each other, forming Au nanorod assemblies in a large area with high density. The assembly of nanorods on the silicon substrate was probably due to the shape-selective packing effect induced by capillary force during solvent evaporation.[35] The superiority of side-by-side aligned Au nanorods over end-to-end tubes can be attributed to the transverse capillary force exceeding the longitudinal capillary force.[35] Additionally, the rods' transverse capillary force is much stronger than the spherical particle's lateral capillary force, preventing spheres from intermixing in a transverse direction.

Metal nanorods exhibit both transverse and longitudinal surface plasmon (TSP and LSP) resonances that give both transverse and longitudinal plasmon absorption.[23] Figure 2 shows the UV-Vis spectra of gold nanorod solutions with different aspect ratios. For the nanorod samples, two absorption bands are observed. The first absorption band appears at about 520 nm, which should be attributed to the TSP absorption. The other band caused by the LSP resonance red-shifts from 746 nm to a high wavelength region with the increase of aspect ratio. For nanorods with aspect ratio of 31.6, no LSP absorption band was observed in UV-Vis regions because the LSP absorption band fell in the near-infrared regions. Note that the surface plasmon absorption of the spherical particles (aspect ratio 1) shifts from about 520 nm to 531 nm. The red-shift of the surface plasmon adsorption band for spherical nanoparticles can be attributed to the aggregation of the nanoparticles.

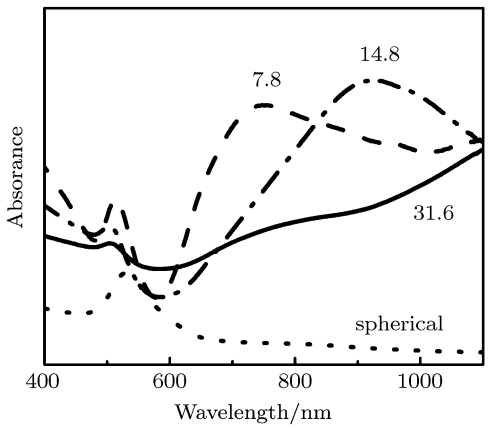

Fig. 2. UV-Vis spectra of as-prepared gold nanorod solutions differing in aspect ratio: (a) 31.6, (b) 14.8, (c) 7.8, (d) 1, indicating that the nanorod exhibits TSP and LSP absorption bands and the LSP absorption band red-shifts with the increase of aspect ratio.

The crystal structure of the Au nanorods was characterized by X-ray diffraction (XRD). Figure 3 shows the XRD patterns of Au nanorods self-assembled on the Si substrate. The Au nanorods were 14.8 and 7.8 in aspect ratio, respectively. The XRD patterns show typical fcc structured crystalline structures of Au that are consistent with the standard XRD pattern of Au (JCPDS No. 04-0784). It is worth noting that the ratios between the intensities of the (111) and (200) diffraction peaks for nanorods with aspect ratios of 14.8 and 7.8 are 4.3 and 5.0, respectively, which is much higher than the conventional value of 2.5, indicating that the nanorods have abundant {111} facets. This is consistent with the fact that their {111} planes tend to be orientated parallel to the surface of the supporting substrate.[36]

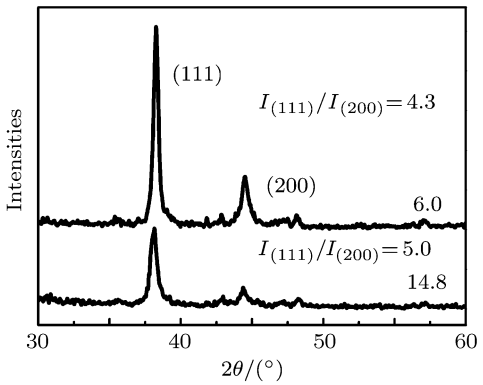

Fig. 3. XRD patterns of gold nanorods with aspect ratios of 7.8 and 14.8. The intensity of (111) and (200) diffraction peaks for Au nanorods is much higher than the standard value, indicating that the nanorod samples have abundant (111) facets.

3.2. Effect of varying aspect ratios of gold nanorods on SERS

The SERS spectra of ordered gold nanorod arrays with different rod aspect ratios were investigated using 2-NAT and R6G as model molecules. The two molecules were chosen because they have a high affinity to the gold atom and each of these molecules has a large Raman cross section, which gives a large contribution to SERS.[37] Figures 4(a) and 4(b) show the SERS spectra of 2-NAT and R6G molecules adsorbed on ordered gold nanorod arrays with different aspect ratios, and the Raman scattering (RS) spectrum of the corresponding powder samples. Compared with the RS spectra of powders, the Raman signals for the two molecules adsorbed on Au nanorod array substrate are dramatically enhanced. In Fig. 4(a), the vibration bands at 1380 cm^{-1} (ring stretching) and 767 cm^{-1} (ring deformation) are observed in both SERS and RS spectra for 2-NAT, indicating that 2-NAT molecules have been adsorbed on the Au/Si substrate.[13,38] Moreover, three obvious differences in SERS and RS spectra are also found in Fig. 4(a). First, all Raman signals of 2-NAT molecule on Au nanorod arrays and Au NPs substrate show great enhancement. Second, a C–H bending mode at 1083 cm^{-1} in the RS spectrum shifts to 1066 cm^{-1} in all the SERS spectra. This can be explained by the fact that 2-NAT binds perpendicularly to the metal surface, thereby preferentially enhancing and shifting the vibration mode at 1066 cm^{-1}. Finally, the C–S stretching mode overlapped with ring deformation shifts from 355 cm^{-1} to 367 cm^{-1} (not shown), which can be attributed to the formation of S–Au bond. In addition, the signal intensity change for the peak at 1566 cm^{-1} was different from that at either 1582 or 1619 cm^{-1}. The signal intensities for bands at 1582 and 1619 cm^{-1} were obviously enhanced in SERS, while for the peak at 1567 cm^{-1}, almost no increase was observed, which are in good agreement with Aroca's results of A.[9] Assuming that the 2-NAT molecular

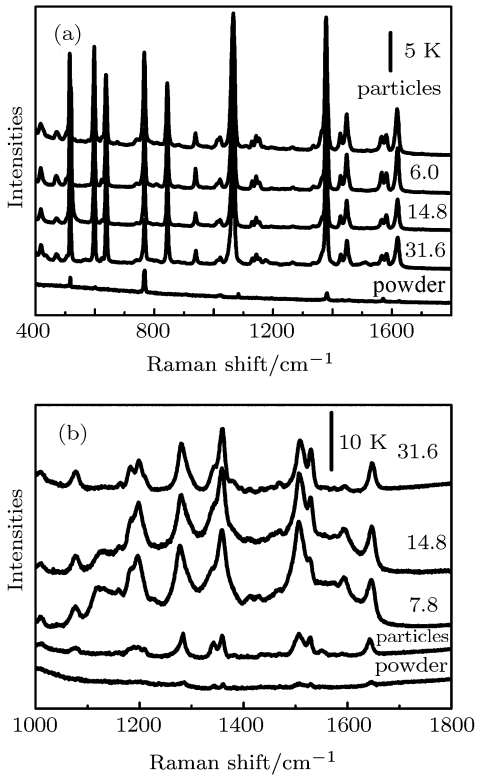

Fig. 4. SERS of (a) 2-NAT and (b) R6G at 1×10^{-3} M using gold nanorods with different aspect ratios, 31.6, 14.8, 7.8 and 1. Raman spectra of 2-NAT and R6G powders were also recorded (the bottom curve). Gold nanorods show an enhancing effect on both molecules.

plane was perpendicular to the substrate surface could explain this difference. The elongation of the C=C

stretching was normal to the substrate surface for the 1619 cm^{-1} band and also, although to a less extent, for the 1582 cm^{-1} mode. The mode at 1567 cm^{-1} was attributed to C=C stretching almost parallel to the substrate surface.

The SERS spectrum for R6G on Au nanorods with different aspect ratios and the RS spectrum for R6G are shown in Fig. 4(b). Similar to that of 2-NAT, Raman signals for R6G were dramatically enhanced on the nanorod substrates. The characteristic bands for R6G were all observed on the SERS spectrum. The strong bonds in Fig. 4(b) at 1360, 1507 and 1646 cm^{-1} correspond to the aromatic C=C double bond stretching modes. The obvious band at 1278 cm^{-1} in all the SERS spectra being attributed to the C–O–C stretching vibration was observed,[39,40] indicating that R6G molecules are adsorbed on the nanorod substrate.

It is interesting that different signal intensities of SERS from nanorods are found with different aspect ratios (Fig. 4). The Raman signal intensity of SERS increases with decreasing aspect ratio. The best substrate for SERS for both target molecules was found to be the Au nanorods with the aspect ratio of 7.8. The signal intensity of SERS from spherical nanoparticles was the weakest of all samples. For a better understanding of the aspect ratio dependence of enhancement effect for highly ordered self-assembled nanorods, we calculated the surface enhancement factors (f_e) for nanorods of different aspect ratios using:[32]

$$f_e = \frac{I_{SERS}}{I_{Raman}} \times \frac{M_{bulk}}{M_{ads}},$$

where M_{bulk} is the number of molecules sampled in the bulk, M_{ads} is the number of molecules adsorbed and sampled on the SERS active substrate, I_{SERS} is the intensity of a vibrational mode in the surface-enhanced spectrum and I_{Raman} is the intensity of the same mode in the Raman spectrum. For the spectra of 2-NAT, the symmetric C–H bending vibration mode ($\sim$ 1066 cm^{-1}) was preferentially enhanced and employed to calculate f_e values. In addition, for R6G, aromatic C=C double bond stretching modes (1646 cm^{-1}) were selected in order to calculate surface enhancement factor values. M_{bulk} was estimated by using the bulk density and the molecular weight of the model molecule: for 2-NAT the bulk density was 1.1 $g{\cdot}cm^{-3}$ and the molecular weight was 160.2 $g{\cdot}mol^{-1}$, and for R6G they were 0.87 $g{\cdot}cm^{-3}$ and 479.02 $g{\cdot}mol^{-1}$, respectively. The number of molecules sampled in the SERS experiments was determined by calculating the total two-dimensional area occupied by the nanoparticles in the illuminated laser spot on the surface.[31] This number is calculated using the number of nanoparticles in the illuminated surface, the surface area of each nanoparticle (dependent on the particle size and aspect ratio) to give the total SERS surface area sampled, which is multiplied by the bonding density of model molecules in a SAM, $\sim$0.5 $nmol/cm^{-2}$.[41]

Table 1. Surface enhancement factors for analytes (10^{-3} M) on assemblies of Au nanorods with different rod aspect ratios.

Aspect ratios	2-NAT	R6G
31.6	3.7×10^5	2.1×10^5
14.8	3.8×10^5	3.7×10^5
7.8	5.3×10^5	3.9×10^5
1 (spheres)	6.8×10^4	1.2×10^4

The estimated surface enhancement factors for each of these substrates are shown in Table 1. Spherical nanoparticles with a diameter of about 30 nm show the smallest enhancement factor, about an order of magnitude lower than the rod samples, agreeing well with a previous result.[32] This must be caused by the lightning rod effect. That is, particles with sharp edges have a stronger enhancement effect than those without sharp edges. Another result is that the enhancement factor for nanorods decreases with increasing aspect ratio. Presently, it is well established that noble metal nanostructures exhibit locally enhanced electric fields when illuminated at their localized surface plasmon wavelength [16] and the main contribution to the SERS enhancement effect arises from this local electromagnetic field. If noble metal nanostructures are assembled in close proximity, their surface plasmon resonances are coupled together, resulting in larger electric-field enhancements in the small gap between neighboring nanoparticles.[17,18] When the assembled metal nanoparticles are used as SERS substrates, dramatic variations in the degree of enhancement, often by many orders of magnitude, have been observed. Based on Mie theory, Voshchinnikov and Farafonov[42] have developed a numerical implementation of the extinction and scattering cross-sections, providing a useful tool for understanding nonspherical nanoparticles. When the aspect ratio increases, the longitudinal dipole plasmon resonance red shifts.[43] This result has been confirmed by UV-Vis measurements. The plasmon resonance wavelength was gradually away from the exciting wavelength and the local electromagnetic field becomes smaller when illuminated by the 785 nm laser line. Therefore, the Raman signal intensity decreases with the increase

of aspect ratios. In order to verify the applicability of SERS to trace analysis, we used different concentrations of model molecules as analytes, adsorbed on the substrate with an aspect ratio of 7.8. Figures 5(a) and 5(b) show the SERS spectroscopy for the two molecules at various concentrations. SERS vibrational spectra were quite consistent at different concentrations of the model molecules. The data show an enhancement effect at low molecule concentrations: 2-NAT concentration was 1.0×10^{-9} M and for R6G, 1.0×10^{-7} M. This suggests that the Au substrate is promising for applications in ultrasensitive analysis and detection.

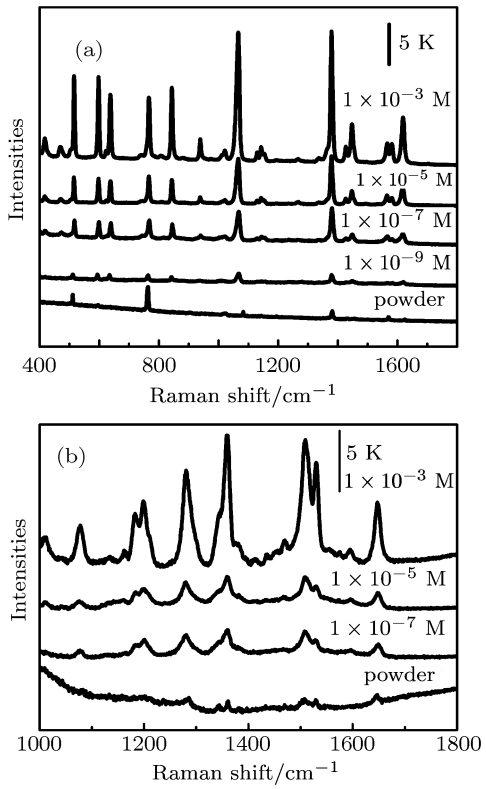

Fig. 5. SERS of (a) 2-NAT and (b) R6G at different concentrations with nanorods of aspect ratio 7.8 as substrate. Raman spectra of 2-NAT and R6G powders were also recorded (the bottom curve). The nanorod substrates exhibit an enhancement effect on the molecules in low concentrations.

4. Conclusion

SERS spectra of 2-NAT and R6G on highly ordered self-assembled gold nanorod arrays were investigated with samples differing in rod aspect ratio. It was found that the enhancement factor decreases with the increase of aspect ratio. The model molecules show an enhancement attributed to the Au nanorods, even at very low concentration, and the enhancement factor at low concentration for either molecule was several orders of magnitude higher than that at high concentrations. These Au nanorod assemblies can serve as high performance SERS substrates.

References

[1] Alekseeva A V, Bogatyrev V A, Dykman L A, Khlebtsov B N, Trachuk L A, Melnikov A G and Khlebtsov N G 2005 *Appl. Opt.* **44** 628
[2] Yu C and Irudayaraj J 2007 *Anal. Chem.* **79** 572
[3] Malic L, Cui B, Veres T and Tabrizian M 2007 *Opt. Lett.* **32** 3092
[4] Nikoobakht B and El-Sayed M A 2003 *J. Phys. Chem.* A **107** 3372
[5] Gole A, Orendorff C J and Murphy C J 2004 *Langmuir* **20** 7117
[6] Laurent G, Félidj N, Aubard J, Lévia G, Krenn J R, Hohenau A, Schider G, Leitner A and Aussenegg F R 2005 *J. Chem. Phys.* **122** 011102
[7] Huff T B, Tong L, Zhao Y, Hansen M N, Cheng J X and Wei A 2007 *Nanomedicine* **2** 125
[8] Aslan K, Lakowicz J R and Geddes C D 2005 *J. Phys. Chem.* B **109** 6247
[9] Alvarez-Puebla R A, dos Santos Jr D S and Aroca R F 2004 *Analyst* **129** 1251
[10] Nie S M and Emory S R 1997 *Science* **275** 1102
[11] Michaels A M, Nirmal M and Brus L E 1999 *J. Am. Chem. Soc.* **121** 9932
[12] Krug J T, Wang G D, Emory S R and Nie S M 1999 *J. Am. Chem. Soc.* **121** 9208
[13] Emory S R and Nie S M 1997 *Anal. Chem.* **69** 2631
[14] Doering W E and Nie S M 2002 *J. Phys. Chem.* B **106** 311
[15] Emory S R, Haskins W E and Nie S M 1998 *J. Am. Chem. Soc.* **129** 8009
[16] Zhang S Z, Ni W H, Kou X S, Yeung M H, Sun L D, Wang J F and Yan C H 2007 *Adv. Funct. Mater.* **17** 3258
[17] Sabur A, Havel M and Gogotsi Y 2008 *J. Raman Spectrosc.* **39** 61
[18] Çlha M C, Kahraman M, Tokman N and Türkoglu G 2008 *J. Phys. Chem.* C **112** 10338
[19] Michaels A M, Jiang J and Brus L 2000 *J. Phys. Chem.* B **104** 11965
[20] Schwartzberg A M, Grant C D, Wolcott A, Talley C E, Huser T R, Bogomolni R and Zhang J Z 2004 *J. Phys. Chem.* B **108** 19191
[21] Jiang J, Bosnick K, Maillard M and Brus L 2003 *J. Phys. Chem.* B **107** 9964
[22] Kim T, Lee K, Gong M S and Joo S W 2005 *Langmuir* **21** 9524
[23] Ueno K, Mizeikis V, Juodkazis S, Sasaki K and Misawa H 2005 *Opt. Lett.* **30** 2158
[24] Gou L F and Murphy C J 2005 *Chem. Mater.* **17** 3668
[25] Lee K S and El-Sayed M 2006 *J. Phys. Chem.* B **110** 19220
[26] Lee K S and El-Sayed M A 2005 *J. Phys. Chem.* B **109** 20331
[27] Tridib K S and Arun C 2004 *Langmuir* **20** 3520
[28] Yang Y, Matsubara S, Nogami M, Shi J L and Huang W M 2006 *Nanotechnology* **17** 2821
[29] Link S and El-Sayed M 1999 *J. Phys. Chem.* B **103** 8410

[30] Chaneya S B, Shanmukh S, Dluhy R A and Zhao Y P 2005 *Appl. Phys. Lett.* **87** 031908
[31] Orendorff C J, Gearheart L, Janaz N R and Murphy C J 2006 *Phys. Chem. Chem. Phys.* **8** 165
[32] Orendorff C J, Gole A, Sau T K and Murphy C J 2005 *Anal. Chem.* **77** 3261
[33] Jana N R, Gearheart L and Murphy C J 2001 *J. Phys. Chem.* B **105** 4065
[34] Xu Z C, Shen C M, Xiao C W, Yang T Z, Zhang H R, Li J Q, Li H L and Gao H J 2007 *Nanotechnology* **18** 115608
[35] Xu Z C, Shen C M, Xiao C W, Yang T Z, Chen S T, Li H L and Gao H J 2006 *Chem. Phys. Lett.* **432** 222
[36] Sun Y G and Xia Y N 2002 *Science* **298** 2176
[37] Maryuri R and Haes A J 2008 *J. Am. Chem. Soc.* **130** 14273
[38] Shen C M, Hui C, Yang T Z, Xiao C W, Tian J F, Bao L H, Chen S T, Ding H and Gao H J 2008 *Chem. Mater.* **20** 6939
[39] Hildebrandt P and Stockburger M 1984 *J. Phys. Chem.* **88** 5935
[40] Lu Y, Liu G L, Kim J, Mejia Y X and Lee L P 2005 *Nano Lett.* **5** 119
[41] Taylor C E, Pemberton J E, Goodman G G and Schoenfisch M H 1999 *Appl. Spectrosc.* **53** 1212
[42] Voshchinnikov N V and Farafonov V G 1993 *Astrophys. Space Sci.* **204** 19
[43] Kelly K L, Coronado E, Zhao L L and Schatz G C 2003 *J. Phys. Chem.* B **107** 668